Polymer Chemistry

Accepted Manuscript

ROYAL SOCIETY OF CHEMISTRY

www.rsc.org/polymers

Cite this: DOI: 10.1039/c0xx00000x

www.rsc.org/xxxxxx

ARTICLE TYPE

Diels-Alder crosslinked HA/PEG hydrogels with high elasticity and fatigue resistance for cell encapsulation and articular cartilage tissue repair

Feng Yu,[a,b] Xiaodong Cao,[*a,b] Yuli Li,[a,c] Lei Zeng,[a,c] Jiehua Zhu,[a,b] Gang Wang,[a,c] and Xiaofeng Chen,[*a,b,c]

The rapid restoration or regeneration of cartilage tissue biomechanical function remains a challenge, especially emphasizing on the replication of structural and mechanical properties using novel scaffold designs. A new class of cross-linked hydrogels with significantly improved mechanical properties has been synthesized by Diels–Alder (DA) click reaction, which is widely used in drug delivery, sensor technology, and tissue engineering. However, the long gelation time of DA formed hydrogel is a big obstacle for cell encapsulation and restricts its application in cytobiology field. In this research, a novel biological hydrogel was synthesized from hyaluronic acid (HA) and PEG by DA "click" chemistry. Through simply tuning the furyl to maleimide molar ratio and the substitution degree of the furyl group, the value of compressive modulus was controlled from 4.86±0.42 kPa to 75.90±5.43 kPa and the gelation time could be tuned from 412min to 51min at 37°C. Moreover, the DA formed hydrogel was firstly utilized to investigate the cell encapsulation viability and the influence of gelation time on encapsulated cells survival, and the results showed that gelation time of about 1h was suitable for cell viability, proliferation and chondrogenesis. Meanwhile, the HA/PEG hydrogel owned outstanding load-bearing and shape recovery properties even after 2000 loading cycles that mimicked the mechanical properties and behaviors of articular cartilage. Therefore, the DA crosslinked HA/PEG hydrogel with good mechanical properties and short gelation time has great potential applications in cartilage tissue engineering.

Introduction

Articular cartilage lesions generally do not heal, or heal only partially under certain biological conditions due to the lack of blood supply and extracellular matrix secretion[1-4]. Many strategies for developing tissue-engineered cartilage have used hydrogels as cell carriers. Hydrogels or injectable hydrogels may serve as scaffolds which provide a more appropriate environment that closely mimics chondrognesis in vivo to guide differentiation of chondrocytes and/or their progenitor cells, resulting in newly formed cartilage tissue[5-7]. However, it has been proved difficult to effectively recreate the biomechanical functions of the natural articular cartilage tissue in these injectable hydrogels at a short-term culture[8, 9]. As we all know, the function of articular cartilage is to support and distribute loads and to provide lubrication in the diarthrodial joints[1, 9]. Meanwhile, the transportation of nutrient in articular cartilage tissue is also dependent on the load-bearing process[10]. Therefore, a hydrogel with intrinsic biomimic mechanical properties and behaviors of articular cartilage was particularly demanded in the field of cartilage tissue engineering[11]. The hydrogel with poor mechanical properties are doomed to failed repair due to the uneven force loading[12, 13].

Diels-Alder (DA) click reaction was investigated as a cross-linking mechanism for hydrogels in last two decades particularly because of its thermal reversibility, mild reaction conditions, catalyst-free and highly efficiency[14-18]. The DA formed hydrogels played a vital role in many biomedical areas such as drug delivery, sensor technology, and tissue engineering[18-21]. A latest literature showed that DA formed degradable PEG hydrogel owned well-defined structural network and the complex shear modulus value was controlled from 2821±1479 Pa to 37097±6698 Pa[22]. Ninh et al had synthesized the reconfigurable shape-memory polyester elastomers via DA coupling and the tensile Young's modulus ranged from 4 to 34 Mpa, which is higher than the most of traditional hydrogels[23]. These novel classes of DA formed hydrogels have potential utility as mechanically robust biomaterials for articular cartilage tissue repair.

Generally, a gelation time of several hours or days is necessary at room temperature for DA formed hydrogels, which is too long for cells encapsulation and limits its application in biologically relevant systems[24-26]. In our previous work, an injectable HA/PEG hydrogel was formed by integrating the DA reaction and enzymatic crosslinking. The gelation time was reduced to several minutes for cell encapsulation but with partly sacrifice of mechanical properties[27]. In this work, we aimed at reducing the gelation time of HA/PEG hydrogel to a suitable level by simply tuning the furyl to maleimide molar ratio and the substitution degree of the furyl group in the premise of good mechanical performance.

We anticipated obtaining the optimum gelation time for cell encapsulation and the cell viability could be maintained. At the same time, the chemical and physical properties were also discussed carefully to make sure that Diels-Alder click chemistry

is an efficient crosslinking method to form hydrogel with enhanced mechanical properties for articular cartilage tissue repair. Since HA had been proved for maintaining chondrocyte viability, supporting and promoting the chondrogenic differentiation of MSCs[28-32], in this case we choose HA as a main component to form hydrogels by DA click chemistry and hope that the robust HA/PEG hydrogel is biocompatible to encapsulate the cells and benefit to promote the ATDC-5 cells chondrogenesis.

Materials and methods

1 Material

Hyaluronic acid sodium (M_w = 1×10^6) was purchased from Shanghai crystal pure industrial Co., LTD (Shanghai, China). 2-morpholinoethane sulfonic acid (MES), 4-(4, 6-dimethoxy-1, 3, 5-triazin-2-yl)-4-methylmorpholiniumchloride (DMTMM) and furylamine were purchased from Sigma-Aldrich (Guangzhou, China). Dimaleimide poly (ethylene glycol) (MAL-PEG-MAL) (M_w = 2×10^3) was purchased from Shanghai Sunway Pharmaceutical Technology Co., LTD (Shanghai, China). All other reagents and solvents were of analytical grade and used as received.

2 Methods

2.1 Synthesis of HA-furan and HA/PEG hydrogel

Furyl-modified HA (HA-furan) was synthesized according to the reported procedures[19, 20, 33]. Briefly, HA (500 mg, 1.25 mmol carboxyl groups) was dissolved in 150 mL of MES buffer (100 mM, pH 5.5), in which DMTMM (1.4 g, 5 mmol; 0.7 g, 2.5 mmol; 0.35 g, 1.25 mmol) was added to active the polysaccharide carboxyl groups for 10min. Subsequently, furylamine (220 μL, 3 mmol (DS1); 110 μL, 1.5 mmol (DS2); 55 μL, 0.75 mmol (DS3)) was added dropwise by using a pipette, and kept stirring at room temperature for another 24h. After that, it was dialyzed against distilled water for 3 days (M_w cut-off 1.4×10^4). Finally, HA-furan derivative was obtained as a white porous sponge by lyophilization.

Lyophilized HA-furan was resuspended in PBS or ultrapure water at a concentration of 1.5% w/v, and allowed to fully hydrate for 24 h at room temperature with stirring. The MAL-PEG-MAL (the mole ratio of furyl to maleimide was controlled at 1:1, 3:1 and 9:1) was added into the solution for 5min and the mixed solution was injected into a cylindrical mould to form the gel at different temperature. The final hydrogels were labeled as DS1 1:1, DS1 3:1, DS1 9:1, DS2 1:1, DS2 3:1, DS2 9:1, DS3 1:1, DS3 3:1, DS3 9:1. Due to the low substitute degree of HA-furan and low concentration of MAL-PEG-MAL, the hydrogel DS3 9:1 couldn't be obtained.

2.2 The morphology and gelation time of HA/PEG hydrogels

The morphology of HA/PEG hydrogel at swollen state was observed by a light microscope (Eclipsc Ti-U, Japan Nikon). The freeze-dried hydrogels was observed using a scanning electron microscope (SEM) (Quanta 200, Netherlands FEI) after being gold-coated in a sputter coater (Sanyo Denshi, Japan).

The gelation time of hydrogels was determined at different temperature using a test tube inverting method as reported by Jeong et al[34].

2.3 Mechanical properties

Compressive modulus of hydrogels was measured using dynamic mechanical analyzer (DMA Q800 USA) with unconfined compression mode. These swollen hydrogels were cut into cylinders (the height was of about 5 mm and diameter was of 10 mm). In order to obtain the values of stress-at-failure and strain-at-failure, linear ramp force of 1 N/min was loaded on the hydrogels until the hydrogel break. As the initial surface of the cylindrical sample was not perfectly flat, the strain from 10% to 15% was used to determine the value of compressive modulus[35]. The storage modulus and the loss modulus were obtained by changing the frequency from 0.1 to 10 Hz and keeping the amplitude of 25 μm[36]. In order to investigate the shape recovery and anti-fatigue properties, the hydrogels were exposed to two kinds of cyclic testing regimes. The first one was that the samples were under 4 cycles of ramp force loading and unloading[37, 38]. The loading and unloading rate was 1 N/min and -1 N/min respectively. The other regime was that the samples were under periodic 20 kPa compressive stress and maintained for 3s between loading and unloading cycles, where more than 2000 consecutive cycles were performed for each hydrogel sample.

2.4 Swelling property

To examine the swelling properties, the DA cross-linked hydrogel samples were prepared in a cylindrical mould according to above procedure. The samples were immersed into the PBS (100 mM, pH 7.4) at 37°C for 48h until the equilibrium of swelling had been reached. The swollen hydrogels were weighed after the excess of water on the surfaces was absorbed with a filter paper. The swelling ratio was calculated using the following equation:

$SW = (W_s - W_d) / W_d$

Where W_s and W_d are the weights of the hydrogels at equilibrium swelling state and freeze-dried state, respectively.

2.5 ATDC-5 cells encapsulation and cell viability

ATDC-5 cells, a murine chondrocytic cell line, were widely used as a culture system to study chondrogenic differentiation[39]. In vitro cell viability was evaluated by encapsulating the ATDC-5 cells at a density of 8×10^5 cells/100 μL in each 100 μL hydrogel. The freeze-dried HA-furan was firstly exposed to Cobalt 60 irradiation for sterilization and dissolved in sterile culture medium. After gelling, the hydrogels were immediately incubated in Dulbecco's modified Eagle's medium (Gibco) (DMEM) and Ham's F12 (1:1) with 10% fetal bovine serum. The live-dead assay (Live-Dead assay Kit (Invitrogen)) of the cells in the above samples was observed by a fluorescence microscope (Eclipsc Ti-U, Japan) to investigate the relationship of gelation time and cell viability. The living cells were stained green and the dead cells were stained red. The ATDC-5 cells were encapsulated in hydrogels with three different gelation time (6h, 3h and 1h) which labeled as GT 6h, GT 3h and GT 1h. In order to investigate the cell proliferation, the CCK-8 staining was performed using 10% (total medium volume) of CCK-8 solution and an incubation time of 3 h. And then the OD value at 450nm was measured using Thermo 3001 microplate reader (Thermo, USA) (n=4).

2.6 Gene expression

Total RNA was extracted from hydrogel at each time point by using the TRIzol® Reagent (Invitrogen). Briefly, hydrogels were transferred into TRIzol® Reagent and homogenized via power homogenizer. Incubate the homogenized samples for 5 minutes at room temperature to permit complete dissociation of the

nucleoprotein complex. The samples were centrifuged at 12000×g for 15 minutes at 4°C after adding the chloroform. The mixture separated into a lower red chloroform phase, an interphase, and a colorless upper aqueous phase. The aqueous phase which contained RNA was transferred into a new tube. The RNA was precipitated by adding the isopropanol and centrifuged at 12000×g for 10 minutes at 4°C. In the end, the RNA was washed by 75% ethanol twice and resuspended in RNase-free water for the next reverse transcription. The resuspended total RNA was reverse transcribed to cDNA in a 10 μL reaction using the PrimeScript® RT reagent Kit with gDNA Eraser following kit instructions (TaKaRa). Real-time PCR was performed using SYBR® *Premix Ex Taq*™ II (TaKaRa). Gene expression of collagen type II and aggrecan was determined relative to the expression of housekeeping gene glyceraldehyde-3-phosphatase dehydrogenase (GAPDH)[40-44]. The sequence of primers for GAPDH, type II collagen and aggrecan were as follows (forward and backward, 5′ to 3′):

GAPDH: 5′-TGTGTCCGTCGTGGATCTGA-3′, 5′-TTGCTGTTGAAGTCGCAGGAG-3′;

Type II collagen gene: 5′-AGGGCAACAGCAGGTTCACATAC-3′, 5′-TGTCCACACCAAATTCCTGTTCA-3′;

Aggrecan: 5′-AGTGGATCGGTCTGAATGACAGG-3′, 5′-AGAAGTTGTCAGGCTGGTTTGGA-3′;

A widely used method to present relative gene expression is the comparative C_t method also referred to as the $2^{-\Delta\Delta Ct}$. Where $\Delta C_t = (C_{t\ \text{gene of interest}} - C_{t\ \text{internal control}})$, $\Delta\Delta C_t = (C_{t\ \text{gene of interest}} - C_{t\ \text{internal control}})_{\text{experiment group}} - (C_{t\ \text{gene of interest}} - C_{t\ \text{internal control}})_{\text{control group}}$[45].

2.7 Statistical Analysis

Data are expressed as mean ± standard deviation. Statistical significance was determined by analysis of variance (single factor) with $p<0.05$.

3 Results and discussion

3.1 Characterization of HA-furan and HA/PEG hydrogel

The synthesized HA-furan was characterized by ^{1}H-NMR (Bruker AVANCE 400 MHz)[20]. In Fig.S1, the peaks at 6.26, 6.46, 7.41 ppm (furan protons) and 1.9 ppm (N-acetyl glucosamine of HA) were labeled by red rectangle. The spectra showed that furyl group was successfully grafted to HA. The substitution degree (SD) of HA-furan was calculated by comparing the integrated areas of furan protons peaks to that of the N-acetyl glucosamine peak. The SD of HA-furan were respectively of 75.9±5.4%, 53.8±7.8%, and 35.3±5.7%.

The formed HA/PEG hydrogels were all transparent. In Fig.S2A, the letters of A and B can be clearly seen through the hydrogels DS1 9:1 and DS1 1:1, respectively. The cell behaviors in this transparent hydrogel will be observed easily via light microscope compared with opaque hydrogel. Fig.S2B shows the light microscope images of hydrogel DS1 1:1 in the swollen state. The uniform fiber network structure can be seen in the hydrogel. Fig.S2C shows the SEM image of the freeze-dried hydrogel DS1 1:1. The pore size was about 150-250 μm, which was suitable for nutrients and metabolic products flowing in and out as a porous scaffold[46]. The freeze-drying process produced the obvious pore and the fiber was squeezed as flake due to the ice crystal growth. The homogenous pore size of network demonstrated the uniformity and crosslinking availability of the DA hydrogel, which has a significant effect on improving the mechanical properties.

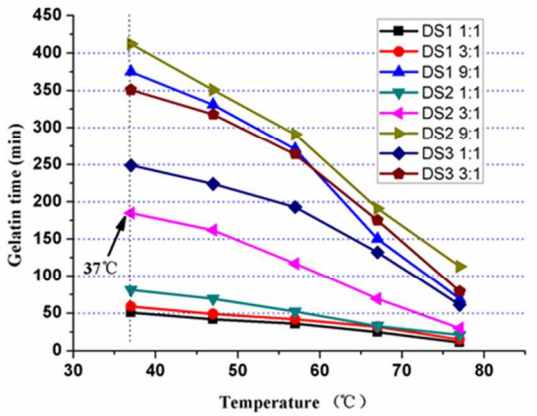

Figure 1. The dependence of gelation time on temperature in different DA formed HA/PEG hydrogels.

3.2 Gelation time

The gelation time of the hydrogels at different temperature was shown in Fig.1. It could be seen that the gelation time decreased sharply with the increase of temperature. This could be explained by that Diels-Alder reaction is a thermal induced chemistry and the higher temperature leads to a faster reaction rate[25, 26, 47, 48]. In this work, the gelation time at 37 °C was discussed carefully in consideration of the hydrogel application in cell-based tissue engineered field. The gelation time could be tuned from 412 to 51 min by simply changing the furyl to maleimide molar ratio and the substitution degree of the furyl group. As we know that the different ratios of reagents have no effect on the kinetic rate of DA reaction. At the same temperature, the DA reaction rate is constant. So the different gelation times were directly decided by the number of effective crosslinking sites formed at the same period.

In the gelling process, the number of crosslinking sites keeps increasing. The gelation time is the point that water is locked in the network and losing of liquidity. The different reagents ratios play an important role on the number of effective crosslinking sites. For the hydrogels DS1 1:1, DS2 1:1 and DS3 1:1, the mole ratio of furan to maleimide is constant, but the substitution degree of furyl functional groups decreases, namely the concentration of furyl functional groups decreases correspondingly. In the same reaction time, the collision reaction probability of two functional groups is obvious higher in hydrogel DS1 1:1 than the other two. As a conclusion, both higher substitution degree of the furyl group and higher concentration of crosslinker MAL-PEG-MAL resulted in a decreased gelling time because of the more existed reactive site. The minimum gelation time was only 51min (hydrogel DS1 1:1), which was a shorter time than the reported hydrogels based on DA reaction[17, 22, 24].

But it's not clear whether this gelling time scope could be

Cite this: DOI: 10.1039/c0xx00000x

www.rsc.org/xxxxxx

ARTICLE TYPE

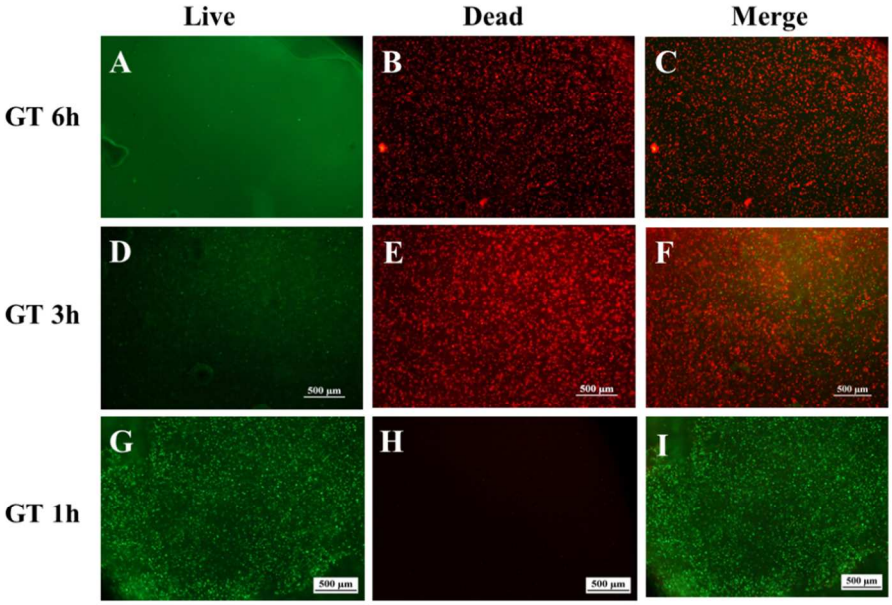

Figure 2. Fluorescence microscope images of live (green), dead (red) and merge images of ATDC-5 cells encapsulated in HA/PEG hydrogels. (A, B, C) The cells were firstly encapsulated into hydrogel DS3 3:1 undergoing 6h gelation time (GT 6h). (C, D, E) The cells were encapsulated into hydrogel DS2 3:1 undergoing 3h gelation time (GT 3h). (G, H, I) The cells were encapsulated into hydrogel DS2 1:1 undergoing 1h gelation time (GT 1h). The culture medium was supplied after gelling process finished. The entire live-dead assays were done after 1 day culture.

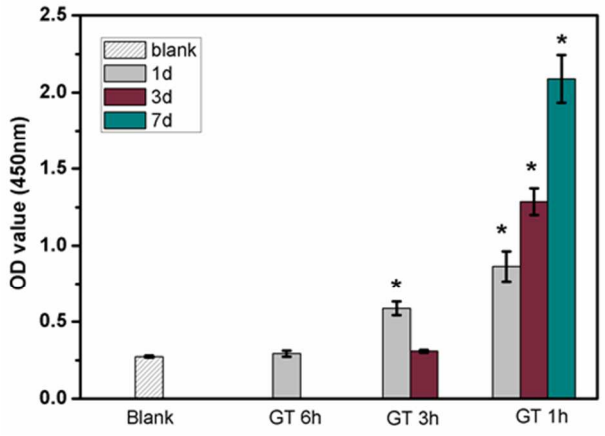

Figure 3. CCK-8 cytotoxicity assay was performed to evaluate the cells proliferation after 1, 3 and 7 days culture. The hydrogel without encapsulated cells was culture at CCK-8 solutions as blank control group. Bars represent the mean ± standard deviation for n=3 samples.

suitable for cell encapsulation and survival or not. And still now no related literatures were reported to discuss the relationship of gelation time and cell viability. According to the gelation time at 37°C, hydrogels DS1 1:1, DS1 3:1 and DS2 1:1 were classified as GT 1h due to similar gelling time. In the same way, the hydrogel DS2 3:1 and DS3 1:1 were classified as GT 3h and the remaining hydrogels were GT 6h. Three kinds of gelation time were utilized to testify which one was optional for cell encapsulation.

3.3 Relationship of gelation time and cell viability

In order to demonstrate the relationship of gelation time and cell live-dead behavior, the hydrogels of GT 1h, GT 3h and GT 6h were chosen to encapsulate the ATDC-5 cells. The culture medium was supplied after gelling process and the fluorescence microscope images were captured after 1 day culture. Fig.2 shows the live-dead behavior of ATDC-5 cells. When the gelation time was 6h, the ATDC-5 cells encapsulated in the hydrogel DS3 3:1 all died (shown in Fig.2B) and no living cells existed (shown in Fig.2A) after 1 day culture because of the long gelation time and the lack of nutrition supply. In Fig.2D and E, a part of living cells and amount of dead cells could be seen after 1 day culture in GT 3h hydrogel. The percentage of dead cells was obviously higher than that of living cell in the merge image Fig. 2F. Fortunately, in hydrogels GT 1h, a different phenomenon was observed from Fig.2H, the number of dead cells was almost neglected compared with hydrogels GT 3h and GT 6h. It demonstrated that the hydrogel GT 1h was the most suitable one for cell survival.

Fig.3 showed the relationship of gelation time with cell proliferation behavior. It can be seen that there was no cells survival in hydrogels GT 6h via comparing with the blank control group after 1 day culture. The blank control groups were hydrogels without cells. For hydrogels GT 3h, an increasing OD value suggested a certain number of living cell existed on first day. But on the third culture day, the OD value also reduced to the level of blank control. That could be explained by that a

Cite this: DOI: 10.1039/c0xx00000x

www.rsc.org/xxxxxx

ARTICLE TYPE

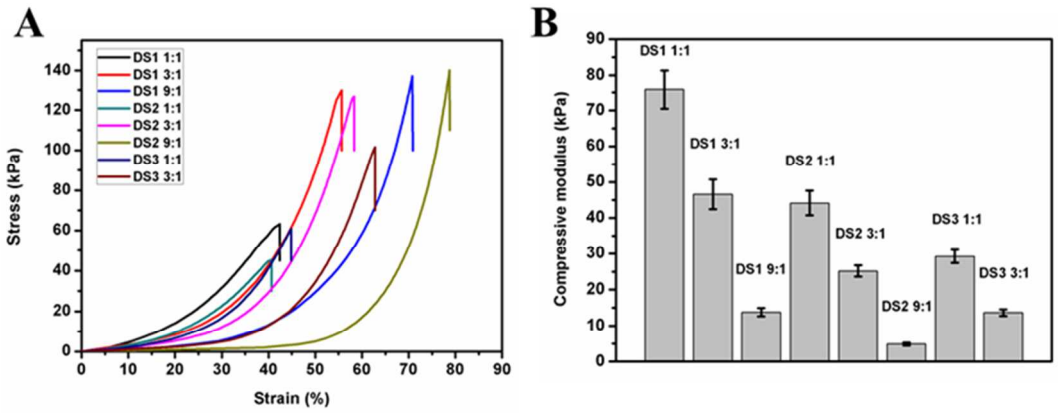

Figure 4. (A) Typical compressive stress-strain curves for HA/PEG hydrogels. (B) The compressive modulus of the hydrogels.

certain number of dead cells in hydrogels would continually promote the living cells apoptosis. But in hydrogels of GT 1h, the significant increasing of OD value testified the obvious proliferation behavior even after 7 days culture. The cell live-dead assay and proliferation results shown in Fig.2 and Fig.3 demonstrated that the hydrogels of GT 1h were more suitable for cell encapsulation and survival.

3.4 Mechanical properties

Hydrogel samples were tested for their mechanical properties under compression. From the resulting compressive stress-strain plots (Fig.4A), the compressive modulus, stress-at-failure, strain-at-failure values were determined. The substitution degree and mole ratio of furan to maleimide had a big effect on the stress-strain behavior and compressive modulus. From the Fig.4B, it could be seen that higher furyl substitution degree led to higher elastic modulus when the mole ration of furan to maleimide was constant (e.g. compressive modulus DS1 1:1 >DS2 1:1 > DS3 1:1). Meanwhile, the compressive modulus decreased as the mole ratio of furan to maleimide increasing (e.g. compressive modulus DS1 9:1 < DS1 3:1 <DS1 1:1). For example, the hydrogel DS2 9:1 owned the highest value of strain-at-failure (76.9±2.3%) and stress-at-failure (139.4±14.8 kPa). But the compressive modulus was the lowest of about 4.86±0.42 kPa. For hydrogel DS1 1:1, the compressive modulus at 75.90±5.43 kPa was the highest among all of the hydrogels. But its values of strain-at-failure (41.2 ± 1.5%) and stress-at-failure (62.1 ± 4.3 kPa) were the lowest.

Considering only the hydrogels of GT 1h were suitable for cell encapsulation, the mechanical properties of hydrogels DS1 1:1, DS1 3:1 and DS2 1:1 need to be investigated further. By comparing the three hydrogels, the hydrogel DS1 3:1 owned higher compressive strain (60%) and breaking strength (130 kPa). However hydrogel DS1 1:1 and DS2 1:1 both possessing the minimum breaking strength (40-60 kPa) and breaking strain (30-40%) were more brittle than DS1 3:1. It has been reported that articular cartilage will recover its initial dimensions even after millions of load bearing due to the elasticity of the solid matrix, the increased osmotic pressure within the tissue and the imbibition of the fluid within the interstitium[9, 37]. Therefore, the hydrogel DS1 3:1 with more excellent elasticity was suitable for articular cartilage load-bearing.

The characterization of shape recovery and anti-fatigue properties of hydrogel DS1 3:1 after every load removal was necessary. Two kind of cyclic testing regimes were exposed to hydrogel samples. As shown in Fig. 5A, the hydrogel samples were under 4 cycles of ramp force loading and unloading at rate of 1N/min. There was a hysteresis loop occurred in every cycle between loading curve and unloading curve. It demonstrated the energy dissipation after each cycle. The second, third and fourth cycles were almost elastic with slightly smaller amount of hysteresis. But they all closely followed the path of the first unloading curve and no significant difference among them. It clearly demonstrated that the hydrogel owned good shape recovery property[38, 49, 50]. In order to further prove the anti-fatigue property of hydrogel DS1 3:1, the second cyclic testing regime was used and the hydrogels were holding more than 2000 cycles. In Fig. 5B, the deformation of hydrogel was recovered completely from about 30% to 0% after each 3 seconds rest at the beginning. Along with the increase of cycles, the unrecovered strain was slowly increasing and the compressive strain also had a slightly increasing trend due to the reasonable accumulation of internal friction in hydrogels (shown in Fig. 5C). They maintained resilience greater than 83% even after 2000 cycles. These could be explained that the equidistant PEG molecular segments as well as proper crosslinking density leads to uniform structural network to resist and recovery the compress deformation. It's a schematic of one compressive cycle for hydrogel and the network deformation in Scheme 1. The equidistant PEG molecular segments could be seen as the elastic walls to block the loss of water within the hydrogel network. The PEG molecule segments was maintained a contractive state without compression, but under compression situation, the pressure caused by interstitial water lead to PEG segments stretching and bending toward to the unconfined edge. The reversible contracting and stretching state of PEG molecular

Cite this: DOI: 10.1039/c0xx00000x

www.rsc.org/xxxxxx

ARTICLE TYPE

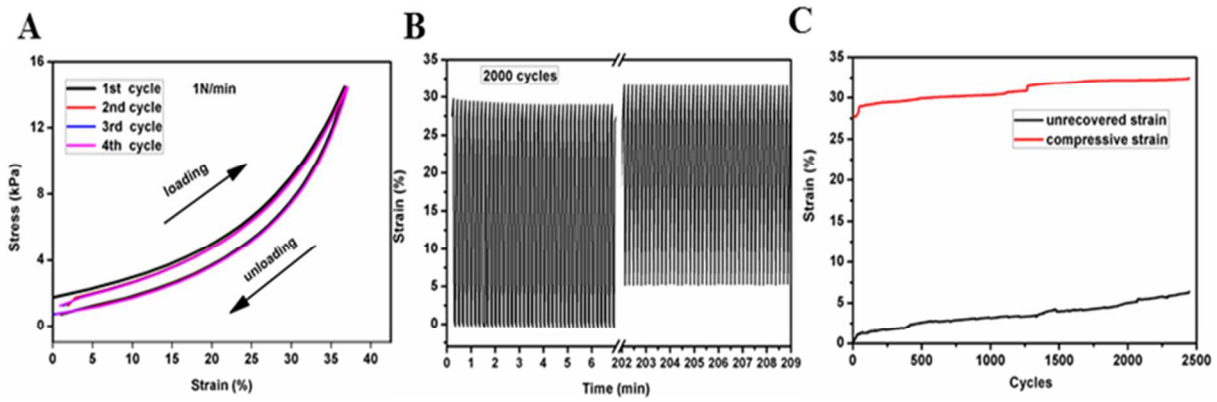

Figure 5. (A) Four successive loading/unloading cycles of hydrogels. The ramp force loading rate and unloading rate was 1 N/min and -1 N/min. (B) Strain recovery property of the hydrogels under 2000 cycles of force loading and unloading. (The every loading stress was kept at 20 kPa) (C) The variation tendency of hydrogel's compressive strain and unrecovered strain after 2500 loading cycles.

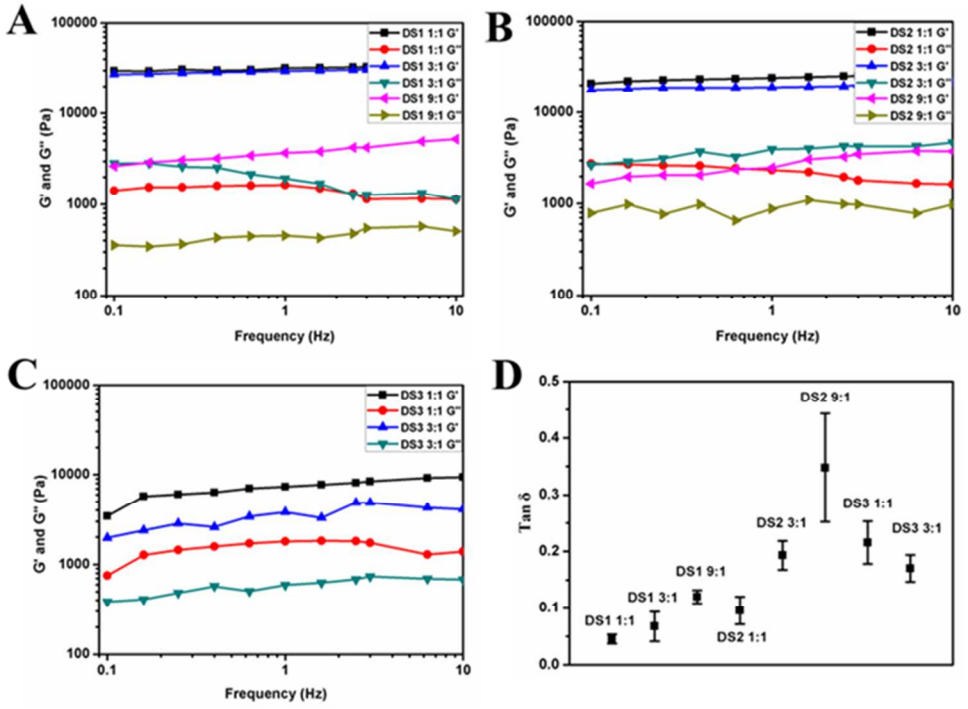

Figure 6. (A, B, C) Storage modulus (G') and loss modulus (G'') of hydrogels. (D) The average tan δ (=G''/G') of the hydrogels.

segments will result in good shape recovery property of hydrogels. All the mechanical characterizations showed that the hydrogel DS1 3:1 owned a rapid shape recovery behavior and an excellent anti-fatigue property which were suitable for articular cartilage tissue repair.

As we know, the lower internal friction resulted in better fatigue resistance. The internal friction of hydrogels was determined by viscoelastic property including the storage modulus G' and loss modulus G''. From Fig.6 (A, B, C), it can be seen that all the hydrogels investigated were predominantly elastic materials with a G' much higher than G'' in a frequency range from 0.1 to 10 Hz. G' and G'' represented the energy stored or dissipated per unit strain[36, 49]. The G' of HA/PEG hydrogels increased from 2.74 ± 0.77 kPa (DS2 9:1) to 31.64 ± 1.54 kPa (DS1 1:1). It demonstrated that the hydrogel DS1 1:1 could store more energy than hydrogel DS2 9:1. In Fig.6D, the hydrogel DS1 3:1 (GT 1h hydrogel) owned the second-smallest loss factor tan δ (=G''/G') which was about 0.07. Given that a tan δ value of zero is

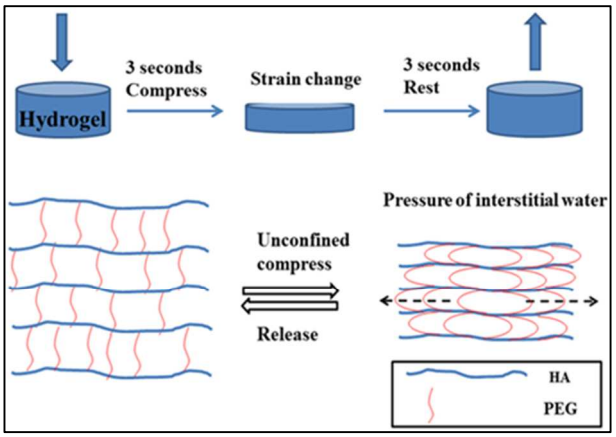

Scheme 1. Schematic diagram of the DA crosslinked HA/PEG network deformation under unconfined compression.

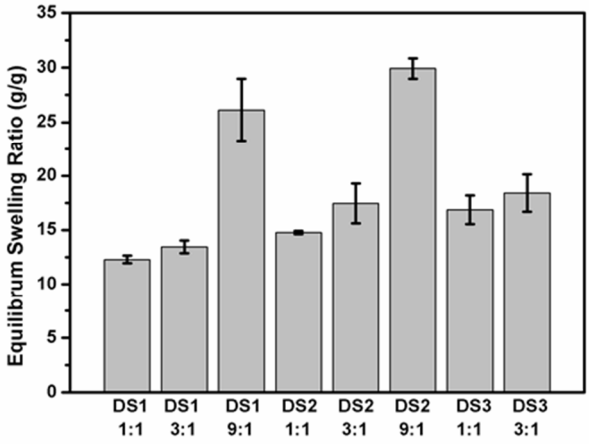

Figure 7. Equilibrium swelling ratio of HA/PEG hydrogels at 37℃.

expected for a perfectly covalent gel without internal friction, this result showed that the proportion of energy that stored elastically in DS1 3:1 was very high compared to that dissipated. That's why the hydrogel DS1 3:1 possessed the outstanding shape recovery and anti-fatigue properties.

3.5 Swelling ratio

The swelling ratio is an important parameter for hydrogels to be used in biomedical fields. Many properties of hydrogels such as mechanical strength and flexibility are mainly associated with their swelling ratio[51]. In Fig.7, all the hydrogels could be highly swollen in water (the swelling ratio >10 g/g), which is a result of hydrophilicity of PEG and HA molecules and maintenance of the crosslinked HA/PEG networks. There was no significant difference between DS1 1:1 and DS1 3:1, DS2 1:1 and DS2 3:1, DS3 1:1 and DS3 3:1. But the swelling ratio of hydrogel DS1 9:1 (26.1±2.8) and DS2 9:1 (29.9±0.9) had a rapidly increase due to the much looser network compared with other hydrogels easily for water absorbing.

3.6 Gene expression of collagen Ⅱ and aggrecan

The productions of matrix proteins by the cells embedded in hydrogel DS1 3:1 with or without TGF-β3 were qualitatively detected with RT-PCR analysis (Fig. S3). From the Fig.S3B and C, the aggrecan and collagen type II transcription levels were significantly increased for +TGF-β3 constructs compared with the constructs cultured in the absence of TGF-β3 at every time point. It was a reasonable result because MSCs were typically induced to chondrogenic differentiation in hydrogel in the presence of transforming growth factor-βs (TGF- βs)[52, 53]. But it was encouraging that hydrogels also exhibited up-regulation of type II collagen and aggrecan in the absence of growth factor TGF-β3which shown in Fig.S3A.The gene expression level of aggrecan had a big increase in the first three weeks. The expression level of controls (day 7) is represented as 1. It can be found that the gene level at 21d was about 170 fold higher than the control. But at the fourth week, there was no significant increase for the aggrecan expression. For type II collagen, the gene expression level was continuously up-regulated until the fourth week. And it was about 35 times higher than control. It could be explained that the bioactive molecular HA played an important role which could support and promote the chondrogenic differentiation of MSCs[29, 30, 32, 54].

4 Conclusions

The DA formed HA/PEG hydrogels with good mechanical properties and short gelation time had been firstly verified in this study. Unlike the traditional DA hydrogels, a series of HA/PEG hydrogels including DS1 1:1, DS1 3:1 and DS2 1:1 used here had an appropriate gelation time for cell encapsulation, survival and proliferation. Among them, the hydrogels DS1 3:1 were the most successful one with high elasticity and fatigue resistance even after 2000 loading cycles. Also, the gene expression levels of collagen Ⅱ and aggrecan were significantly up-regulated either with or without growth factor TGF-β3. We believe that the tunable comprehensive performances will extend this high strength hydrogels to a wide range of applications at the field of articular cartilage repair.

ACKNOWLEDGMENT

This work was financially supported by National Basic Re-search Program of China (973 Program) (Grant NO. 2011CB606204, 2012CB619100), the Specialized Research Fund for the Doctoral Program of Higher Education of China (Grant No. 20110172120002), National Natural Science Foundation of China (Grant No. 51372085, 51202069, 51172073), Program for New Century Excellent Talents in University (NCET-11-0148) and Fundamental Research Funds for the Central Universities (Grant No.2013ZZ0005).

Notes and references

a. School of Materials Science and Engendering, South China University of Technology, Guangzhou, 510641, PR China. Fax: +86-20-87111752; Tel: +86-20-22236066; E-mail: caoxd@scut.edu.cn

b. National Engineering Research Centre for Tissue Restoration and Reconstruction, Guangzhou, 510006, PR China. Fax: +86-20-22236083; Tel: +86-20-22236283; E-mail: chenxf@scut.edu.cn

c. Guangdong Province Key Laboratory of Biomedical Engineering, South China University of Technology, Guangzhou 510640, PR China.

1. A. M. Bhosale and J. B. Richardson, *British Medical Bulletin*, 2008, **87**, 77-95.
2. J. A. Buckwalter, *J Orthop Sports Phys Ther*, 1998, **28**, 192-202.
3. J. A. Buckwalter, *Clin Orthop Relat Res*, 2002, **402**, 21-37.
4. J. A. Buckwalter, H. J. Mankin and A. J. Grodzinsky, *Instr Course Lect*, 2005, **54**, 465-480.
5. J. Elisseeff, *Expert Opin Biol Ther*, 2004, **4**, 1849-1859.
6. X. H. Hu, Y. Zhu and C. Y. Gao, *Progress in Chemistry*, 2009, **21**, 2164-2175.
7. K. L. Spiller, S. A. Maher and A. M. Lowman, *Tissue Engineering Part B-Reviews*, 2011, **17**, 281-299.
8. C. Y. Huang, V. C. Mow and G. A. Ateshian, *J Biomech Eng*, 2001, **123**, 410-417.
9. V. C. Mow and X. E. Guo, *Annual Review of Biomedical Engineering*, 2002, **4**, 175-209.
10. V. C. Mow, M. H. Holmes and W. M. Lai, *J Biomech*, 1984, **17**, 377-394.
11. F. T. Moutos, L. E. Freed and F. Guilak, *Nature Materials*, 2007, **6**, 162-167.
12. B. Balakrishnan and R. Banerjee, *Chemical Reviews*, 2011, **111**, 4453-4474.
13. D. J. Huey, J. C. Hu and K. A. Athanasiou, *Science*, 2012, **338**, 917-921.
14. H.-L. Wei, Z. Yang, Y. Chen, H.-J. Chu, J. Zhu and Z.-C. Li, *European Polymer Journal*, 2010, **46**, 1032-1039.
15. I. Kosif, E.-J. Park, R. Sanyal and A. Sanyal, *Macromolecules*, 2010, **43**, 4140-4148.
16. H.-L. Wei, Z. Yang, H.-J. Chu, J. Zhu, Z.-C. Li and J.-S. Cui, *Polymer*, 2010, **51**, 1694-1702.
17. E. Goiti, M. B. Huglin and J. M. Rego, *European Polymer Journal*, 2004, **40**, 219-226.
18. S. Yigit, R. Sanyal and A. Sanyal, *Chem.-Asian J.*, 2011, **6**, 2648-2659.
19. H. Tan, J. P. Rubin and K. G. Marra, *Macromolecular Rapid Communications*, 2011, **32**, 905-911.
20. C. M. Nimmo, S. C. Owen and M. S. Shoichet, *Biomacromolecules*, 2011, **12**, 824-830.
21. K. C. Koehler, K. S. Anseth and C. N. Bowman, *Biomacromolecules*, 2013, **14**, 538-547.
22. S. Kirchhof, F. P. Brandl, N. Hammer and A. M. Goepferich, *Journal of Materials Chemistry B*, 2013, **1**, 4855-4864.
23. C. Ninh and C. J. Bettinger, *Biomacromolecules*, 2013, **14**, 2162-2170.
24. W. Hong-Liang, Y. Jun, C. Hui-Juan, Y. Zhe, M. Cun-Cai and Y. Kai, *Journal of Applied Polymer Science*, 2011, **120**.
25. Y.-L. Liu, C.-Y. Hsieh and Y.-W. Chen, *Polymer*, 2006, **47**, 2581-2586.
26. H.-L. Wei, Z. Yang, L.-M. Zheng and Y.-M. Shen, *Polymer*, 2009, **50**, 2836-2840.
27. F. Yu, X. Cao, Y. Li, L. Zeng, B. Yuan and X. Chen, *Polymer Chemistry*, 2014.
28. Amos Matsiko, Tanja Levingstone, Fergal J. O'Brien and J. P. Gleeson, *Journal of the Mechanical Behavior of Biomedical Materials*, 2011, **11**, 41-52.
29. C. Chung, M. Beecham, R. L. Mauck and J. A. Burdick, *Biomaterials*, 2009, **30**, 4287-4296.
30. C. Chung, J. Mesa, G. J. Miller, M. A. Randolph, T. J. Gill and J. A. Burdick, *Tissue Engineering*, 2006, **12**, 2665-2673.
31. K. Lindenhayn, C. Perka, R. S. Spitzer, H. H. Heilmann, K. Pommerening, J. Mennicke and M. Sittinger, *Journal of Biomedical Materials Research*, 1999, **44**, 149-155.
32. W. S. Toh, T. C. Lim, M. Kurisawa and M. Spector, *Biomaterials*, 2012, **33**, 3835-3845.
33. F. Yu, X. Cao, L. Zeng, Q. Zhang and X. Chen, *Carbohydr Polym*, 2013, **97**, 188-195.
34. B. Jeong, Y. H. Bae and S. W. Kim, *Macromolecules*, 1999, 7064-7069.
35. A. L. Buyanov, I. V. Gofman, L. G. Revel'skaya, A. K. Khripunov and A. A. Tkachenko, *J Mech Behav Biomed*, 2010, **3**, 102-111.
36. J. J. Roberts, A. Earnshaw, V. L. Ferguson and S. J. Bryant, *Journal of Biomedical Materials Research Part B-Applied Biomaterials*, 2011, **99B**, 158-169.
37. I. C. Liao, F. T. Moutos, B. T. Estes, X. Zhao and F. Guilak, *Advanced Functional Materials*, 2013, **23**, 5833-5839.
38. D. C. Tuncaboylu, A. Argun, M. Sahin, M. Sari and O. Okay, *Polymer*, 2012, **53**, 5513-5522.
39. R. S. Tare, D. Howard, J. C. Pound, H. I. Roach and R. O. C. Oreffo, *European Cells and Materials* 2005, **10**, 22.
40. J. D. Kisiday, P. W. Kopesky, C. H. Evans, A. J. Grodzinsky, C. W. McIlwraith and D. D. Frisbie, *J Orthop Res*, 2008, **26**, 322-331.
41. L. H. Nguyen, A. K. Kudva, N. L. Guckert, K. D. Linse and K. Roy, *Biomaterials*, 2011, **32**, 1327-1338.
42. L. H. Nguyen, A. K. Kudva, N. S. Saxena and K. Roy, *Biomaterials*, 2011, **32**, 6946-6952.
43. G. D. Nicodemus and S. J. Bryant, *Journal of Biomechanics*, 2008, **41**, 1528-1536.
44. G. D. Nicodemus, I. Villanueva and S. J. Bryant, *Journal of Biomedical Materials Research Part A*, 2007, **83A**, 323-331.
45. T. D. Schmittgen and K. J. Livak, *Nat. Protocols*, 2008, **3**, 1101-1108.
46. D. J. Griffon, M. R. Sedighi, D. V. Schaeffer, J. A. Eurell and A. L. Johnson, *Acta Biomater*, 2006, **2**, 313-320.
47. N. W. Polaske, D. V. McGrath and J. R. McElhanon, *Macromolecules*, 2009, **43**, 1270-1276.
48. N. W. Polaske, D. V. McGrath and J. R. McElhanon, *Macromolecules*, 2011, **44**, 3203-3210.
49. A. H. Milani, A. J. Freemont, J. A. Hoyland, D. J. Adlam and B. R. Saunders, *Biomacromolecules*, 2012, **13**, 2793-2801.
50. J. Cui, M. A. Lackey, A. E. Madkour, E. M. Saffer, D. M. Griffin, S. R. Bhatia, A. J. Crosby and G. N. Tew, *Biomacromolecules*, 2012, **13**, 584-588.
51. Y. Xiao, L. He and J. Che, *Journal of Materials Chemistry*, 2012, **22**, 8076-8082.
52. C. Chung and J. A. Burdick, *Tissue Engineering Part A*, 2009, **15**, 243-254.
53. R. L. Mauck, S. B. Nicoll, S. L. Seyhan, G. A. Ateshian and C. T. Hung, *Tissue Eng*, 2003, **9**, 597-611.
54. M. Akmal, A. Singh, A. Anand, A. Kesani, N. Aslam, A. Goodship and G. Bentley, *J Bone Joint Surg*, 2005, **87-B**.

Table of Contents Graphic

The gelation time of Diels-Alder crosslinked HA/PEG hydrogels could be reduced to an appropriate level for cell encapsulation and survival. Meanwhile, the DA click reaction made the gel to be highly resilient and capable of resisting cyclic compression loading which biomimic the native articular cartilage biomechanical functions.